

Scalable Multi-Robot Motion Planning Using Guidance-Informed Hypergraphs

Courtney McBeth¹, James Motes¹, Isaac Ngui¹, Marco Morales¹, and Nancy M. Amato¹

Abstract—In this work, we present a multi-robot planning framework that leverages guidance about the problem to efficiently search the planning space. This guidance captures when coordination between robots is necessary, allowing us to decompose the intractably large multi-robot search space while limiting risk of inter-robot conflicts by composing relevant robot groups together while planning. Our framework additionally supports planning with kinodynamic constraints through our conflict resolution structure. This structure also improves the scalability of our approach by eliminating unnecessary work during the construction of motion solutions. We also provide an application of this framework to multiple mobile robot motion planning in congested environments using topological guidance. Our previous work has explored using topological guidance, which utilizes information about the robots’ environment, in these multi-robot settings where a high degree of coordination is required of the full robot group. In real-world scenarios, this high level of coordination is not always necessary and results in excessive computational overhead. Here, we leverage our novel framework to achieve a significant improvement in scalability and show that our method efficiently finds paths for robot teams up to an order of magnitude larger than existing state-of-the-art methods in congested settings with narrow passages in the environment.

I. INTRODUCTION

Multi-robot systems are becoming increasingly prevalent in settings like warehouses and factories where it is important to be able to quickly find collision-free paths for robot teams. These often constrained environments require careful motion planning for each robot to accomplish its task without collision. Some navigation approaches compute individual paths for each robot and resolve conflicts online; however, in congested environments, this introduces the risk of deadlock. Here, we consider the problem of multi-robot motion planning which resolves inter-robot conflicts during the offline planning stage.

Similarly, decoupled offline multi-robot motion planning (MRMP) methods [1] plan for each robot separately and provide no coordination during planning, making them unsuitable for overly constrained environments. On the other end of the spectrum, coupled methods [1] plan for all robots together in the *composite space*, the joint planning space of all robots. These methods have full knowledge of each robot’s configuration at all times and thus do provide the high

level of coordination required to solve difficult problems. However, the size of the composite space is exponential in the number of robots, making these methods computationally intractable for large robot teams.

Hybrid methods [2]–[4] provide a mix of decoupled and coupled planning to provide scalability along with an increased level of coordination during planning when necessary. The Decomposable State Space Hypergraph (DaSH) [5] framework presents a general structure for hybrid planning that benefits from a sparse representation of the planning space. This representation models when coordination between robots is needed, allowing the planner to stay in low-dimensional search spaces when possible, and captures the connections between these spaces. The framework features a hierarchical approach consisting of a high-level representation of the planning space that guides construction of an optimistic motion solution, which is then validated. The DaSH framework can be applied to develop methods for a variety of multi-robot planning problems.

DaSH proposes an approach to exhaustively constructing the high-level representation of the planning space that performs well for problems like multi-manipulator rearrangement [5], where the search space has an exploitable structure since actions can be classified as pick, place, handoff, etc., but becomes intractable for real-world problems which lack this highly structured search space, such as mobile robot motion planning. Our insight is that we can leverage information about the planning problem to induce this structure while building the high-level representation of the planning space and further exploit this guidance to efficiently search the planning space. As such, we propose *Guided-DaSH*, an adaptation to the DaSH framework to support a wider range of real-world problems. Our framework adapts each level of DaSH, including the conflict resolution structure, which allows our approach to support planning under kinodynamic constraints and limit unnecessary work while constructing the motion solution. We additionally present *Workspace Guided-DaSH*, an application of our Guided-DaSH framework to the problem of multiple mobile robot motion planning in environments with narrow passages where the workspace is used to guide the composition decisions.

Sampling-based motion planning methods, which sample robot configurations to find a path, struggle with the *narrow passage problem*, referring to the difficulty of exploring tight areas of the environment. Considering multi-robot systems, this problem is exacerbated by the need to avoid both obstacle and inter-robot collisions. Prior work [6]–[9] has explored using workspace guidance to direct planning

¹Courtney McBeth, James Motes, Isaac Ngui, Marco Morales, and Nancy M. Amato are with the Parasol Lab, Department of Computer Science, University of Illinois Urbana-Champaign, Champaign, IL 61820 USA {cmcbeth2, jmotest2, ingui2, moralesa, namato}@illinois.edu

This work was supported in part by the IBM-Illinois Discovery Accelerator Institute and the Center for Networked Intelligent Components and Environments (C-NICE) at the University of Illinois.

through narrow passages. We recently introduced *Composite Dynamic Region-biased RRT* (CDR-RRT) [10], a coupled MRMP method that leverages topological guidance to efficiently plan paths in congested environments with narrow passages. CDR-RRT provides the high level of coordination required to resolve complex inter-robot conflicts while its use of topological guidance limits its exploration of the composite space to areas likely to yield a solution. Here, we leverage the structure of the workspace to provide structure to the planning space, informing when coordination between robots is necessary, and to guide planning through narrow passages.

In this paper, we propose *Guided-DaSH*, an adaptation of the DaSH framework to a broader class of multi-robot planning problems. We implement our adapted framework to the problem of multiple mobile robot motion planning in congested environments with narrow passages to propose *Workspace Guided-DaSH*, a MRMP method guided by knowledge of the physical environment the robots exist within. Our contributions include:

- An adaptation of the DaSH framework to multi-robot planning problems without a highly structured search space and a novel hybrid MRMP method built on our adapted framework that leverages the workspace to guide planning in multiple ways.
- Support for a broader range of real-world problems, including planning under kinodynamic constraints within our framework via an adapted conflict resolution structure.
- An extensive experimental validation showing that our novel approach scales to robot groups up to 128, an order of magnitude larger than previous methods.

II. PRELIMINARIES AND PRIOR WORK

In this section, we describe relevant motion planning preliminaries and discuss prior work in the field of multi-robot motion planning.

A. Motion Planning Preliminaries

In motion planning, a *configuration* refers to a set of values for a robot's *degrees of freedom*, including their position in the workspace, orientation, and other parameters such as joint angles. The *configuration space* (C_{space}) consists of all possible configurations and can be partitioned into C_{free} and C_{obst} made up of valid and invalid configurations respectively. Motion planning is the problem of finding a path from a start configuration q_s to a goal configuration q_g through C_{free} . Computing the full C_{obst} is intractable [11], [12], thus state-of-the-art methods turned to sampling-based motion planning [13], [14]. One such method, Rapidly-exploring Random Trees (RRT) [14], iteratively grows a tree made up of configurations and local connections between them until reaching the goal. This method achieves fast exploration of the C_{space} by growing the tree toward randomly sampled configurations. Alternatively, graph-based methods aim to build a *roadmap* graph, a discretized approximation of C_{free} [13], [15], [16].

B. Multi-robot Motion Planning

The multi-robot motion planning problem is an extension of the motion planning problem which consists of finding valid paths $\Pi = \{\pi_{r_1}, \dots, \pi_{r_n}\}$ for a set of robots $R = \{r_1, \dots, r_n\}$ that also avoid inter-robot collision. Multi-agent pathfinding (MAPF) is the discrete state space equivalent of the MRMP problem which consists of finding collision-free paths for a set of robots over a given graph representation (e.g. a grid) rather than through continuous space. In environments with narrow passages, it is non-trivial to construct a graph representation that captures the connectivity of the planning space, hence our consideration of MRMP.

Decoupled methods, such as Decoupled PRM [1], plan paths for each robot separately. These methods are incomplete and, thus, cannot resolve complex inter-robot conflicts. Some coupled methods, including Composite PRM [1] and Composite RRT [14] provide a high level of coordination by planning directly in the composite space, $C_0 \times \dots \times C_{n-1}$ where C_i is the configuration space of robot i . This becomes computationally intractable due to the high dimensionality of the space with large groups of robots. Other coupled methods, including MRdRRT [17] and its variants [18], [19], construct single-robot roadmaps and then use these to search an implicit composite space roadmap.

Hybrid methods seek to leverage the benefits of both decoupled and coupled planning. CBS-MP [2] performs a low-level search to find decoupled paths for each robot and resolves conflicts using a high-level search in the composite space. Several hybrid MAPF methods have been proposed to find collision-free paths given a representation of the C_{space} (e.g. roadmap). M* [3] conducts an A*-like search using a technique called *subdimensional expansion* in which the optimal individual paths for each robot are followed until a conflict occurs. Then, the conflicting agents are merged together and a new conflict-free composite path is found. Subdimensional Expansion RRT (SRRT) [20] applies subdimensional expansion to MRMP. It first constructs individual policies by growing RRTs in the individual C_{space} of each robot backward from the goal. It then expands a tree forward in the composite space by following the individual policies until conflict occurs. Then, new configurations are sampled for expansion in the composite space of the conflicting robots. The Multi-agent Pathfinding with Constraints (MAPF/C) approach [4] annotates the underlying representation with constraints indicating that two robots cannot occupy two vertices, two edges, or an edge and a vertex at the same time. These constraints are then used by a general MAPF method to find conflict-free paths. While these methods perform well in open environments, in constrained settings, they expend excess computation on conflict resolution, limiting planning efficiency.

C. Kinodynamic Motion Planning

Kinodynamic motion planning extends the conventional motion planning problem by incorporating the dynamics of the robotic system. This problem requires finding valid paths that adhere to differential kinematic constraints, which limit

the robot’s position, and differential dynamic constraints, which can bound the robot’s velocity or acceleration. The inclusion of these constraints allows the paths to more accurately reflect the motions of real-world systems.

Kinodynamic planning has been performed with curve parameterization [21], lattice-based [22], and motion primitive [23] based planners, where pre-processing was used to generate a valid set of curves or motion primitives for planning purposes. However, as sampling-based algorithms gained popularity due to their speed and scalability to high-dimensional spaces, they began to be adapted for handling kinodynamic constraints. Modifications of the RRT algorithm integrated the robot’s kinodynamic constraints into the traditional steering functions.

An initial version of the kinodynamic RRT [24] algorithm randomly sampled a control input for the robot and a duration for which the control was to be applied. The dynamics were then integrated forward in time for the sampled duration or until a collision occurred, to obtain the new configuration. Unlike conventional methods that terminate upon connecting to the goal configuration, this approach terminated upon reaching a goal region, accommodating the complexities introduced by sampling in the control space.

Later extensions of the RRT algorithm employed optimal control techniques for steering functions, such as controllers for linear quadratic systems [25], [26], retaining some of the advantageous properties of these well-established methods. The kinodynamic RRT algorithm was further refined to find optimal kinodynamically feasible paths, where the paths were required to satisfy both kinematic and dynamic constraints while achieving asymptotic optimality [27], [28].

Multi-robot extensions of kinodynamic motion planning were later introduced. Building upon the principles of multi-robot motion planning, the Subdimensional Expansion RRT (SRRT) [20] algorithm applies its subdimensional expansion-based method to the kinodynamic planning problem by utilizing splines as its steering function, facilitating expedited planning with kinodynamic constraints. Kinodynamic Conflict-Based Search (K-CBS) [29] extends hybrid MRMP algorithms to accommodate kinodynamic constraints, drawing on the concepts of CBS-MP [2]. This approach introduces kinodynamic conflicts and employs a kinodynamic low-level planner akin to the kinodynamic RRT in [24], enabling the ability to solve high-dimensional problems with general dynamics.

D. Guided Motion Planning

Guided motion planning methods leverage external information to more efficiently find paths. Prior work has explored using knowledge of the workspace to guide planning. The Exploring/Exploiting Tree (EET) algorithm [8] propagates a wavefront expansion through the environment, which it uses to grow a tree from the start to the goal. SyCLoP [9] partitions the environment into workspace decomposition regions, then finds a high-level plan over these decomposition regions from the start region to the goal region. This high-level plan is then used to guide the growth of an RRT through

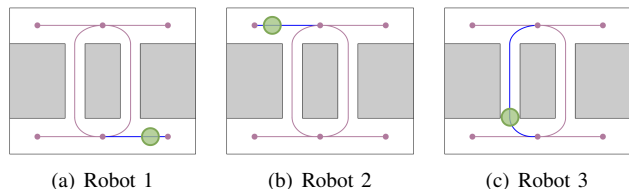


Fig. 1. An example of a composite skeleton edge and a composite region. Each of the three robots has its own workspace skeleton, shown in purple. Three skeleton edges that comprise a composite skeleton edge are shown in blue. Three individual regions that make up a composite region along this composite skeleton edge are shown in green.

\mathcal{C}_{space} . These single-robot approaches show the benefit of utilizing workspace guidance for efficient planning.

1) *Skeleton-Guided Motion Planning*: Skeleton graphs have been built to leverage information about the workspace. A skeleton is an embedded graph in which edges represent free areas of the workspace and vertices represent connections between these areas. Examples include medial axis skeletons [30] and Reeb graphs [31] for 2D environments and mean curvature skeletons [32] for 3D. They are generally quick to compute, for example, medial axis skeletons can be computed in $O(n \log n)$ time where n is the number of obstacle edges [33]. Skeleton-guided motion planning methods [6], [7], [34] use dynamic regions, bounded local areas of the workspace that advance along skeleton edges, to efficiently explore free areas of the environment, including narrow passages. Dynamic Region-biased RRT (DR-RRT) [6], a single-robot motion planning method, initializes a region on the skeleton vertex closest to the start. Then, iteratively, configurations are sampled from within this region and the region is moved forward along its skeleton edge. When it reaches the end of its edge, new regions are spawned on the newly reached outgoing edges. This procedure continues until the goal is reached.

2) *Composite Dynamic Region-biased RRT*: We extended DR-RRT to multi-robot motion planning for scenarios with narrow passages where a high level of coordination during planning is required. Composite Dynamic Region-biased RRT (CDR-RRT) [10] is a coupled method that lazily builds and searches over a *composite skeleton* (Fig. 1), which is the Cartesian product graph of the workspace skeleton for each robot in the group. MAPF is used to generate a path over the workspace skeleton for each robot, taking into account the capacity of each edge as given by the clearance to obstacles in the environment. These paths are then combined to form composite skeleton edges, each of which represents a set of workspace skeleton edges, one per robot. These edges form a path through the composite skeleton. As in DR-RRT, regions advance along these composite skeleton edges, building a tree from the start until the goal is reached. Here, however, the regions exist in the composite space, representing a set of individual regions, one per robot.

Although CDR-RRT shows a significant improvement in scalability compared to other state-of-the-art methods in extremely congested environments with narrow passages

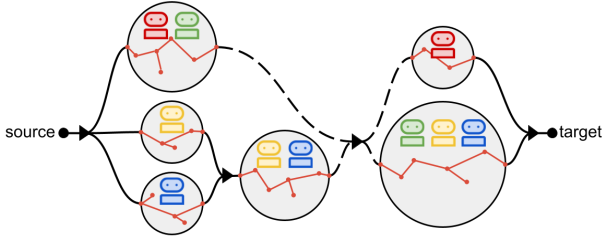


Fig. 2. An example hypergraph representation of a hybrid planning space for a group of four robots. The planner moves between different levels of composition, coupling robots together to resolve conflicts and decoupling them when possible. The orange trees represent an example plan through each space. The dashed hyperarc, for example, represents a change in composition wherein the red robot can now be considered in its own planning space while the green, yellow, and blue robots must now coordinate and are considered jointly.

where coordination between the full robot group is required during planning [10], considering the full composite space of all robots comes with significant computational overhead due to its large size. We now propose a hybrid method extended from CDR-RRT that uses topological guidance to inform when planning in the composite space (of all or just a subgroup of robots) is necessary.

E. Decomposable State Space Hypergraph

The Decomposable State Space Hypergraph (DaSH) framework [5] for hybrid multi-robot planning leverages a hypergraph representation to enable coordination between relevant groups of robots without considering the full composite space unless necessary. A hypergraph $\mathcal{H} = (\mathcal{V}, \mathcal{E})$ is a generalization of a graph where hyperarcs $E \in \mathcal{E}$ represent connections between sets of vertices, the *tail set* containing the source of the hyperarc and the *head set* containing the target [35]. Here, we consider directed hypergraphs, in which hyperarcs represent connections in only one direction from the tail set to the head set. In the original framework, hyperarcs may be bidirectional. A hypergraph representation of the problem space provides the advantage of sparsity. While an equivalent graph could be constructed, vertices would need to represent a value for every robot in the problem, leading to a combinatorial explosion as the number of robots increases. The hypergraph representation; however, only includes relevant robots in each vertex or hyperarc, allowing groups of robots to be composed and decomposed as needed.

The DaSH framework consists of three components: construction of the task space hypergraph, construction of the motion hypergraph, and the query. The *task space* consists of the set of robots and constraints (e.g. start/goal constraints, path constraints) that make up a problem. It can be decomposed into *task space elements* which contain a subset of the robots and relevant constraints. In the *task space hypergraph*, vertices are task space elements capturing the robots required to coordinate and the relevant constraints. Hyperarcs can be categorized as either *composition*, representing changes in the robots considered and constraints, or *transition*, representing changes in constraints for a fixed set

of robots. These transitions may be as simple as configurations that are valid in both the tail and head set of the hyperarc or more complex paths with additional constraints. Figure 2 shows an example of a task space hypergraph for a hybrid MRMP planning space. During planning, robots are coupled together when necessary and decoupled to improve scalability when possible. This is especially beneficial for sampling-based motion planning where the planning time is impacted by the dimension of the \mathcal{C}_{space} considered. The DaSH framework has been implemented for problems including multi-manipulator rearrangement [5] where the task space is highly structured and task space elements represent modes such as a robot holding an object. Hyperarcs can represent transitions such as handoff operations with grasp constraints. This structure allows the sparse task space hypergraph to be constructed exhaustively. For task spaces without such structure, however, this exhaustive construction becomes intractable.

The task space hypergraph is used to build a low-level *motion hypergraph* encoding motion feasibility. Here, vertices represent configurations and hyperarcs represent changes in composition, transitions between task space elements, and robot movement.

The query phase consists of two parts. First, an *optimistic solution* is found which ensures a valid transition history (i.e. guaranteeing that each robot exists in exactly one place at each point along the solution). Because hyperarcs in the motion hypergraph give a local plan for the subset of robots in the group being considered and do not make assumptions about the locations of the other robots, a scheduled query must then be used to validate the solution in terms of inter-robot collisions by inducing waiting. Considering adapting DaSH to problems without a naturally highly structured task space, each of these components poses a design question, which we discuss in Section III. Additionally, we discuss the modifications to the conflict resolution structure that we make to accommodate kinodynamic planning since we can no longer assume the robots are able to instantaneously change velocity in the scheduled query. These changes allow us to bypass the query stage entirely.

III. GUIDED-DASH

In this section, we describe our adaptation to the DaSH framework, *Guided-DaSH*, and explain the modifications we make to support motion planning problems without a highly structured search space via the use of guidance and to support problems with kinodynamic constraints. Figure 3 shows an overview comparison of Guided-DaSH and the original DaSH framework which we will elaborate on below. Algorithm 1 shows an overview of our framework.

A. Guided High-level Search

In order to provide structure to a problem, the Guided-DaSH framework requires the identification of a guiding space G . To provide useful guidance, G must reflect the structure of the planning space and should be quick to search. For example, in Section IV we propose a method

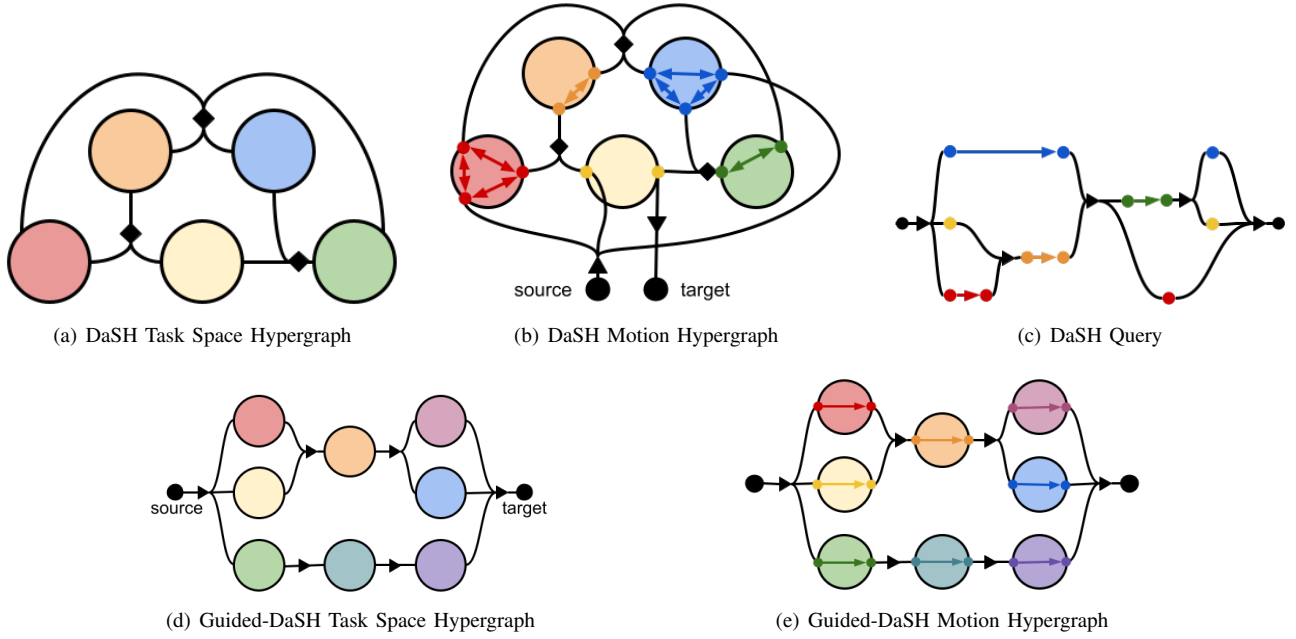


Fig. 3. A comparison of the DaSH framework (a-c) and the Guided-DaSH framework (d-e). In (a-b), diamonds denote undirected hyperarcs. In DaSH, the task space hypergraph (a) and motion hypergraph (b) are exhaustively constructed. The motion hypergraph is then queried to find an optimistic schedule (c) which then undergoes conflict resolution. In Guided-DaSH, the guided search informs which task space elements are necessary, allowing us to build a minimal portion of the task space hypergraph (d) and motion hypergraph (e). Because of this, we can directly extract the motion solution from the motion hypergraph.

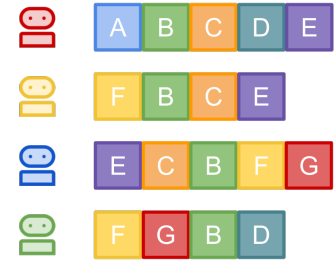
that uses a topological skeleton of the workspace to provide guidance for mobile robot MRMP. Other possible guiding spaces include databases of multi-robot path segments or a discretization of each robot's C_{space} . Identifying this space often requires domain knowledge of the problem being considered.

Each robot configuration should be able to be mapped to a state in G . Thus, when given a query $Q = \{Q_{start}, Q_{goal}\}$ where Q_{start} and Q_{goal} are composite configurations containing start and goal values for each robot, the guided search returns a set of paths $\Pi^G = \{\pi_{r_1}^G, \dots, \pi_{r_n}^G\}$ where each element of the paths is a state in G . The first element of each path is the state in G corresponding to the robot's start configuration and the last element corresponds to its goal. These paths then represent an abstract route that each robot will follow. The query may also be given a set of constraints specifying robots that cannot exist in the same state(s) together. These constraints are informed by the construction of the motion hypergraph and will be described in more detail in Section III-C.

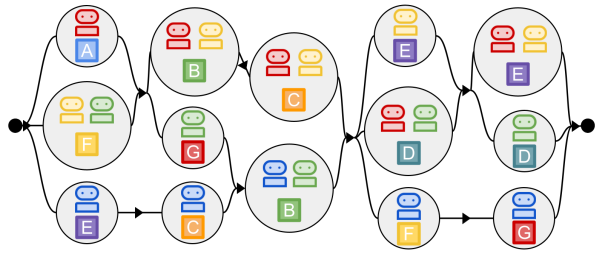
States in G should be defined at a resolution such that robots in the same state likely require coordination to avoid collision or accomplish their task. Using this knowledge, we can leverage Π^G to construct the task space hypergraph.

B. Task Space Hypergraph Construction

The task space hypergraph $\mathcal{H}_{ts} = \{\mathcal{V}_{ts}, \mathcal{E}_{ts}\}$ captures when coordination between robots is necessary. The original DaSH framework [5] exhaustively constructs the task space hypergraph; however, if we use guidance to decide in



(a) Abstract paths over G



(b) Task Space Hypergraph

Fig. 4. Abstract paths over the guiding space G (a) and the constructed task space hypergraph (b) for a 4-robot group. Different colored blocks represent different states in G . As robots move into the same state in G , they are coupled into the same task space element in the task space hypergraph. Task space elements contain a set of robots as well as the constraints associated with the associated state in G .

Algorithm 1 Guided-DaSH

Input: Guiding space G , Query $\{Q_{start}, Q_{goal}\}$

- 1: $\Pi \leftarrow \emptyset$ ▷ Robot motion paths
- 2: $C \leftarrow \emptyset$ ▷ Guided search constraints
- 3: **while** $\Pi = \emptyset$
- 4: $\Pi^G \leftarrow \text{GUIDEDSEARCH}(G, C, Q_{start}, Q_{goal})$
- 5: $\mathcal{H}_{ts} \leftarrow \text{CONVERTTOTASKSPACEHYPERGRAPH}(\Pi^G)$
- 6: $\mathcal{X}_{ts} \leftarrow \text{ORDERBYDEPENDENCY}(\mathcal{H}_{ts})$ ▷ \mathcal{X} is an ordered list of vertices and hyperarcs in \mathcal{H}_{ts}
- 7: $\mathcal{H}_m \leftarrow \emptyset$ ▷ Initialize motion hypergraph
- 8: **for** $x_{ts} \in \mathcal{X}_{ts}$
- 9: $\pi \leftarrow \emptyset$ ▷ Initialize local path
- 10: **if** $X_{ts}.\text{ISVERTEX}$
- 11: $\pi \leftarrow \text{COMPUTEPATH}(G, X_{ts})$
- 12: **else**
- 13: $\pi \leftarrow \text{COMPUTETRANSITION}(G, X_{ts})$
- 14: **if** $\pi = \emptyset$
- 15: $C \leftarrow C \cup \text{GETCONSTRAINT}(X_{ts})$
- 16: **break** ▷ Restart guided search
- 17: $\mathcal{X}_{conf} \leftarrow \text{FINDCOLLISIONS}(\mathcal{H}_m, \pi)$ ▷ Get elements in collision
- 18: **if** $\mathcal{X}_{conf} \neq \emptyset$
- 19: $C \leftarrow C \cup \text{GETCONSTRAINTS}(\mathcal{X}_{conf} \cup \{X_{ts}\})$
- 20: **break** ▷ Restart guided search
- 21: **else**
- 22: $\mathcal{H}_m.\text{ADDPATH}(\pi)$
- 23: $\Pi \leftarrow \text{EXTRACTMOTIONPATHS}(\mathcal{H}_m)$

advance which task space elements are necessary, we can efficiently construct a minimal portion of the task space hypergraph. This makes our adapted framework advantageous for problems where exhaustive construction is computationally intractable. Given the abstract paths for each robot Π^G , we can translate the sequence of states in G that each robot visits into task space elements \mathcal{V}_{ts} and transitions between them \mathcal{E}_{ts} .

Algorithm 2 shows an overview of the task space hypergraph construction procedure. We begin by creating a *virtual source* V_{source} that denotes the start of the problem. Then, at each timestep in the abstract paths, we group together robots in the same state in G and add vertices to the task space hypergraph reflecting that robot group and the constraints associated with the corresponding state in G . Transitions between the previous timesteps and current timesteps are also added. These hyperarcs capture both changes in composition and constraints of the task space elements they connect. Finally, the *virtual target* is added denoting the end of the problem and connected via a hyperarc to the last task space element for each robot. Figure 4 shows an example of this process.

C. Motion Hypergraph Construction

The motion hypergraph \mathcal{H}_m stores the configurations and motions between them that make up the robots' motion paths as well as the composition and transition hyperarcs from \mathcal{H}_{ts} . The abstract paths in G from which \mathcal{H}_{ts} is constructed are only meaningful if the robots' motion paths actually follow the sequence of states Π^G . Thus, it is often necessary to leverage a guided planning method to ensure that the

Algorithm 2 Task Space Hypergraph Construction

Input: Abstract paths $\Pi^G = \{\pi_{r_1}^G, \dots, \pi_{r_2}^G\}$

- 1: $T \leftarrow \max_{r \in R} \|\pi_r^G\|$ ▷ Maximum path timesteps
- 2: $\mathcal{H}_{ts} \leftarrow \{V_{source}, \emptyset\}$ ▷ Initialize task space hypergraph
- 3: $S_{prev} \leftarrow \{(V_{source}, R)\}$ ▷ Previous G state of each robot
- 4: **for** $t \in \{1, \dots, T\}$
- 5: $S_{cur} \leftarrow \emptyset$ ▷ Current G state of each robot
- 6: **for** $r \in R$
- 7: $S_{cur}[\pi_{r,t}^G] \leftarrow S_{cur}[\pi_{r,t}^G] \cup \{r\}$
- 8: **for** $\{state, robots\} \in S_{cur}$
- 9: $\mathcal{H}_{ts}.\text{ADDVERTEX}(\{state, robots\})$
- 10: $\mathcal{E}_{ts} \leftarrow \text{GETTRANSITIONS}(S_{prev}, S_{cur})$
- 11: $\mathcal{H}_{ts}.\text{ADDPHYPERARCS}(\mathcal{E}_{ts})$
- 12: $S_{prev} \leftarrow S_{cur}$
- 13: $\mathcal{H}_{ts}.\text{ADDVERTEX}(V_{target})$ ▷ Connect last vertices to target
- 14: $\mathcal{H}_{ts}.\text{ADDPHYPERARC}(S_{prev}, V_{target})$

constraints associated with each task space element are met when constructing local paths. We detail an example of such as method in Section IV.

For each task space element, a local path is computed in the composite space of the contained therein. These paths become vertices and motion hyperarcs in \mathcal{H}_m . Transition hyperarcs in \mathcal{H}_{ts} must also be translated into local paths. Transitions often require a different method of path construction to account for, e.g., grasp constraints when picking up an object or other factors when moving between states in G .

It is possible that constructing a local path for a task space element or transition could fail. In this case of a task space element failing, a constraint is added to the guided search to prohibit that group of robots from existing in the corresponding state in G together. Similarly, in the case of a transition failing, constraints are added to prevent the groups of robots in the tail and head sets of the transition from being in the corresponding incoming and outgoing states in G together.

In the original DaSH formulation, the entire motion hypergraph is constructed before a scheduled query is performed that finds and resolves conflicts between robot paths through different task space elements or transitions. In our adapted framework; however, since we know from the guided search which task space element's motion should occur concurrently, we can interleave the motion hypergraph construction and conflict detection stages. This allows us to reduce wasted computation by finding conflicts as they occur rather than after the motion hypergraph is constructed which would likely result in local paths being constructed that would not be included in the final paths.

1) *Kinodynamic Planning:* Our modification to the conflict resolution stage also allows us to support kinodynamic planning. The scheduled query proposed in the original DaSH framework resolves conflicts by inducing waiting to prevent robots from colliding with each other. When planning under kinodynamic constraints, we cannot assume the ability of robots to instantaneously change velocity. Additionally, to avoid solving computationally difficult optimal control point-to-point problems, we cannot reuse local paths for task space

elements occurring after conflicts in the robots' paths. Thus, we must replan affected paths to avoid conflicts.

2) *Conflict Detection*: As we construct each movement hyperarc corresponding to motion through a task space element, we track the high-level timestep that this segment of the motion hypergraph corresponds to in the guided search. Additionally, when constructing the movement hyperarcs corresponding to transitions between task space elements, we classify these local paths as extensions of the local paths corresponding to the tail set of task space elements. Then, after each local path is computed, it is checked for collision against each existing local path occurring at the same high-level timestep by considering fine-resolution intermediate configurations along the paths.

When a conflict is found, constraints are added to the guided search to prevent the robots in each task space element or transition from existing in or between the corresponding states in G together. When new constraints are added, the guided search is redone, the task space hypergraph is recomputed, and the construction of the motion hypergraph restarts.

D. Query

The original DaSH framework involves a query stage after the construction of the motion hypergraph to find an optimistic and then a validated schedule of motions for the robots to follow. This is necessary under exhaustive construction of the task space and motion hypergraphs; however, because Guided-DaSH only constructs the portion of the task space hypergraph needed to find a motion solution guided by the abstract paths and resolves conflicts during construction of the motion hypergraph, this stage is no longer necessary. Instead, we can directly extract a motion path for the robots from the computed motion hypergraph and terminate.

IV. WORKSPACE GUIDED-DASH

In this section, we explain how we apply the Guided-DaSH framework for mobile robot MRMP in congested environments with narrow passages to propose the Workspace Guided-DaSH method and describe how we leverage the workspace skeleton representation of the environment to quickly find motion plans for large robot teams. The workspace skeleton functions as the guiding space G and directs both the construction of the task space hypergraph and its translation into the motion hypergraph.

A. Task Space Hypergraph Construction

The task space hypergraph captures when sets of robots should be composed into the same planning space. To construct a meaningful task space hypergraph, we must define the task space elements in a way that captures when coordination between mobile robots is needed. Considering mobile robots, coordination between the motions of robots is required when they are physically in proximity to each other. Our insight is that we can leverage the workspace skeleton to approximate when coordination is necessary by modeling the movement of the robots through the workspace

Algorithm 3 Workspace Guided-DaSH

Input: Skeleton S and a Query $\{Q_{start}, Q_{goal}\}$

- 1: $\Pi \leftarrow \emptyset$ \triangleright Robot motion paths
- 2: $C \leftarrow \emptyset$ \triangleright MAPF search constraints
- 3: **while** $\Pi = \emptyset$
- 4: $\Pi^G \leftarrow \text{MAPF}(S, C, Q_{start}, Q_{goal})$
- 5: $\mathcal{H}_{ts} \leftarrow \text{CONVERTTOTASKSPACEHYPERGRAPH}(\Pi^G)$
- 6: $\mathcal{X}_{ts} \leftarrow \text{ORDERBYDEPENDENCY}(\mathcal{H}_{ts})$ $\triangleright \mathcal{X}$ is an ordered list of vertices and hyperarcs in \mathcal{H}_{ts}
- 7: $\mathcal{H}_m \leftarrow \emptyset$ \triangleright Initialize motion hypergraph
- 8: **for** $x_{ts} \in \mathcal{X}_{ts}$
- 9: $\pi \leftarrow \emptyset$ \triangleright Initialize local path
- 10: **if** $X_{ts}.\text{ISVERTEX}$
- 11: $\pi \leftarrow \text{SIMPLIFIEDCDRRRT}(S, X_{ts})$
- 12: **else**
- 13: $\pi \leftarrow \text{COMPOSITERRT}(X_{ts})$
- 14: **if** $\pi = \emptyset$
- 15: $C \leftarrow C \cup \text{GETCONSTRAINT}(X_{ts})$
- 16: **break** \triangleright Restart guided search
- 17: $\mathcal{X}_{conf} \leftarrow \text{FINDCOLLISIONS}(\mathcal{H}_m, \pi)$ \triangleright Get elements in collision
- 18: **if** $\mathcal{X}_{conf} \neq \emptyset$
- 19: $C \leftarrow C \cup \text{GETCONSTRAINTS}(\mathcal{X}_{conf} \cup \{X_{ts}\})$
- 20: **break** \triangleright Restart guided search
- 21: **else**
- 22: $\mathcal{H}_m.\text{ADDPATH}(\pi)$
- 23: $\Pi \leftarrow \text{EXTRACTMOTIONPATHS}(\mathcal{H}_m)$

Algorithm 4 SIMPLIFIEDCDRRRT

Input: Task space element V , maximum extension failures τ

- 1: $T \leftarrow \emptyset$ \triangleright Initialize empty tree
- 2: $r \leftarrow \text{INITIALIZESAMPLINGREGION}(V.\text{EDGE}.\text{SOURCE})$
- 3: $coveredEdge \leftarrow false$
- 4: **while** $\neg coveredEdge$ and $r.\text{NUMFAILURES} < \tau$
- 5: $q_{rand} \leftarrow \text{SAMPLECFG}(r)$ \triangleright Sample from region
- 6: $q_{new} \leftarrow \text{EXTENDLOCALPATH}(T, q_{rand})$
- 7: **if** $\neg q_{new}.\text{EXTENSIONSSUCCEEDED}()$
- 8: $r.\text{INCREMENTFAILURES}()$
- 9: **else**
- 10: **while** $r.\text{CONTAINSCFG}(q_{new})$
- 11: $r.\text{ADVANCEALONGSKELETONEDGE}(V.\text{EDGE})$
- 12: **if** $r.\text{REACHEDENDOF SKELETONEDGE}(V.\text{EDGE})$
- 13: $coveredEdge \leftarrow true$
- 14: **if** $r.\text{NUMFAILURES} > \tau$
- 15: **return** \emptyset
- 16: **return** T

as movement along the skeleton. Specifically, coordination is necessary when robots are traversing the same skeleton edge (either in the same or opposite direction) or traveling through the same skeleton vertex. A task space element then contains a set of robots and the corresponding segment of the skeleton around which planning is constrained. Transitions model sets of robots moving through the same skeleton vertex. This provides structure to the problem, allowing us to decompose the task space.

Exhaustively constructing the task space hypergraph, which has previously been done for DaSH methods [5], is intractable for the case we consider because the structure we induce on the task space does not allow for as sparse of a task

space hypergraph representation as seen in the previously considered problems. Using the Guided-DaSH framework, we instead construct this representation minimally and as needed by exploiting the guidance provided by the skeleton. We use MAPF to generate abstract paths for the robots to move over the skeleton from the vertex closest to their start to the vertex closest to their goal.

Algorithm 3 shows an overview of Workspace Guided-DaSH. Given a skeleton of the workspace, we first construct a path over the skeleton for each robot using a MAPF algorithm (line 4). We set the capacity of each skeleton vertex and edge as given by the minimum clearance to an obstacle. We then combine these paths to form the minimal necessary portion of the task space hypergraph (line 5). Fig. 5 shows an example of the conversion of the MAPF solution into the task space hypergraph. Robots traversing the same skeleton edge are grouped into the same task space element using composition hyperarcs. As they move away from each other onto different edges, they are decoupled into separate task space elements, boosting planning efficiency by considering smaller C_{spaces} . Transition hyperarcs capture robots moving through the same skeleton vertex, providing the necessary coordination, as well as robots moving between segments of the skeleton (i.e. moving between task space elements with the same robots but different constraints). We then use the task space hypergraph to guide the construction of the motion hypergraph.

B. Translation to Low-level Motion Hypergraph

Once the task space hypergraph is constructed, we compute a set of paths to form the motion hypergraph. The task space hypergraph is only meaningful if the robots roughly follow their abstract paths over the skeleton. We must also traverse narrow passages in the environment. Thus, we leverage the skeleton to guide the construction of local paths along skeleton edges. To compute paths through task space elements, we use a simplified variant of CDR-RRT (Sec. II-D.2; Alg. 3 line 11; Alg. 4) that advances a dynamic region along the skeleton edge.

Considering transition hyperarcs that represent multiple robots moving through a skeleton vertex, we stop the movement of the robots along the incoming skeleton edges a small distance δ from the end of each edge. We’ve found that setting δ to the diameter of the region used for CDR-RRT [10] works well. We then grow an RRT [14] in the composite space of these robots from the last configuration on the robots’ incoming skeleton edges to a sampled configuration at least δ distance away from the skeleton vertex on the robots’ next skeleton edges (Alg. 3, line 13). Here, we simply grow an RRT rather than using CDR-RRT to avoid forcing the robots to reach the skeleton vertex at the same time, creating congestion. Waiting vertices, composition hyperarcs, and transition hyperarcs not associated with movement in the task space hypergraph correspond directly to vertices and hyperarcs in the motion hypergraph.

It is possible for construction of a local path to fail if the RRT fails to be extended a given number of times during

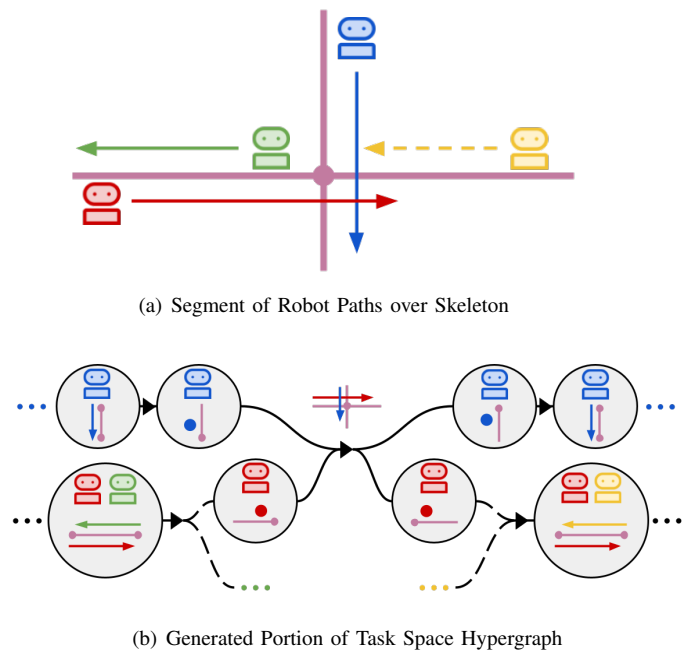


Fig. 5. A segment of the robot paths over the skeleton and the corresponding portion of the task space hypergraph. Each task space element shows the corresponding set of robots and the relevant portion of the topological skeleton. In (b), arrows indicate robots moving along a skeleton edge and dots indicate a decoupled waiting state. Solid lines indicate transition hyperarcs and dashed lines represent composition hyperarcs. The green and red robots are initially moving in opposite directions along the same skeleton edge. Then, red and blue reach the skeleton vertex together and go on to different edges. The yellow robot begins moving in the opposite direction of the red robot when the red robot reaches the next skeleton edge.

planning. In this case, we impose a constraint that the MAPF solution from which we build the task space hypergraph cannot contain the same group of robots traversing along either a skeleton edge that failed or the same groups of robots traversing along the incoming and outgoing skeleton edges to a skeleton vertex that failed (line 15). We then recompute the task space hypergraph and try again to construct a complete motion hypergraph. Similarly, if conflicts are found between robots traversing different portions of the skeleton simultaneously, constraints are imposed to prevent the relevant robot groups from traversing these segments of the skeleton together (line 19).

C. Kinodynamic Planning

Incorporating kinodynamic constraints into Workspace Guided-DaSH is straightforward due to the modularity of the DaSH framework. As kinodynamic constraints primarily influence the motion of the robots, it is imperative that the motion hypergraph construction process accounts for these constraints. To this end, we adapt the Composite-RRT and CDR-RRT algorithms, employed in the construction of the motion hypergraph in Algorithm 3, to incorporate kinodynamic constraints. This is achieved by substituting their underlying RRT with our kinodynamic RRT, following a similar approach to [24].

Algorithm 5 Kinodynamic RRT

Input: Initial State x_0

- 1: $V \leftarrow x_0, E \leftarrow \emptyset, V \leftarrow (V, E)$
- 2: **for** $i = 1 : N$
- 3: $x_{rand} \leftarrow \text{SAMPLE}()$
- 4: $x_{near} \leftarrow \text{NEAREST}(V, x_{rand})$
- 5: $x_{new} \leftarrow \text{KINODYNAMICSTEER}(x_{near}, x_{rand})$
- 6: **if** $x_{new} \neq \text{NULL}$
- 7: $V \leftarrow V \cup x_{new}$
- 8: $E \leftarrow E \cup (x_{near}, x_{new})$
- 9: $G \leftarrow (V, E)$
- 10: **if** $x_{new} \in \text{GoalRegion}$ **return** G

return \emptyset

We model the dynamics of each robot as follows:

$$\dot{x}_i = f_i(x_i, u_i) \quad (1)$$

where $x_i \in \mathcal{X}_i$ represents the state of robot i , and $u_i \in \mathcal{U}_i$ denotes the control input of robot i with \mathcal{X}_i and \mathcal{U}_i being the respective state space and control space of each agent. Drawing on the work presented in [24], we outline our kinodynamic RRT in 5, with the kinodynamic steering function specified in Algorithm 6.

1) *Kinodynamic RRT*: Algorithm 6 begins by sampling a control input for each robot uniformly at random from their respective control space \mathcal{U}_i . The control inputs are sampled either uniformly at random from the control space or by selecting the control that brings the robot closest to the target state x_{rand} . To find the closest control, multiple controls are sampled uniformly at random from the robots' control space and integrated forward in time for a set duration. The control which drives the robot state closest to x_{rand} is used to find x_{new} . Sampling the control in this manner enables effective utilization of the guidance provided by CDR-RRT, as it ensures that the motion is directed as closely as possible toward the direction of the guiding configuration.

Next, a duration to apply the control is sampled with T_{max} being the maximum duration a control can be applied. The control input is then iteratively applied by numerically integrating the robot dynamics forward in time by a single time step, while simultaneously checking for collisions, until the sampled number of steps has been taken. The condition on line 8 of Algorithm 6 ensures that if the robot is steered into an obstacle, the progress made thus far is not retained. This precaution ensures that no future extensions of the tree originate from a vertex that would immediately encounter an obstacle. If no conflicts are encountered, the newly generated node is returned to be added to the RRT. The kinodynamic RRT continues to expand until either a maximum number of states have been added or the goal region has been reached.

V. VALIDATION

We run scaling MRMP scenarios in environments designed to highlight the strengths and weaknesses of Workspace Guided-DaSH (abbreviated *WG-DaSH* in results) relative to other state-of-the-art approaches.

Algorithm 6 KINODYNAMICSTEER

Input: Closest state in tree x_{near} , Target state x_{rand} , Robot dynamics function f , Maximum control duration T_{max}

- 1: $u \leftarrow \text{SAMPLECONTROL}(x_{near}, x_{rand})$
- 2: $k \leftarrow \text{SAMPLEDURATION}(T_{max})$
- 3: $t \leftarrow 0$
- 4: $x_{new} \leftarrow x_{near}$
- 5: **while** $t \leq k$
- 6: $x_{new} \leftarrow \text{INTEGRATE}(f(x_{new}, u))$
- 7: $\text{collision} \leftarrow \text{INCOLLISION}(x_{new})$
- 8: **if** collision **return** NULL
- 9: $t \leftarrow t + \Delta t$

return x_{new}

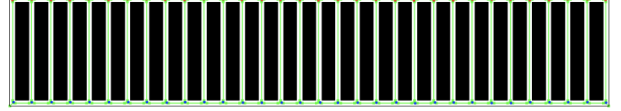
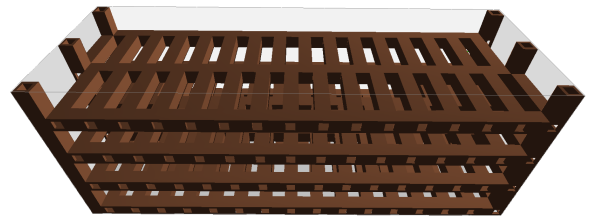


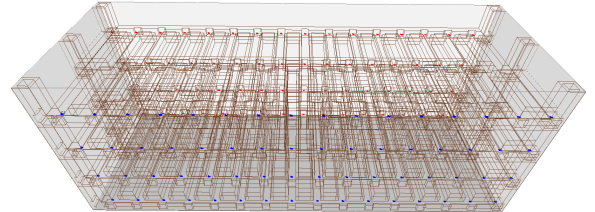
Fig. 6. In the Warehouse environment, robots located on the top and bottom of each narrow aisle must swap places with the robot they are vertically aligned with.

A. Experimental Setup

We measure the performance of Workspace Guided-DaSH against CDR-RRT [10] as well as a set of other approaches that are relevant for comparison. Composite RRT [14] operates in the full composite space, providing a high level of coordination. MRdRRT [17] was originally intended for manipulators, but its implicit search of the composite space makes it pertinent for comparison. SRRT [20] uses subdimensional expansion to limit the size of the search space which is similar in concept to our hypergraph representation. We use Conflict-based Search [36] over the workspace skeleton to perform the guided search for Workspace Guided-DaSH. Each method was implemented in the open-source Parasol Planning Library. All holonomic experiments were



(a) Tunnels Environment



(b) Tunnels Query

Fig. 7. In the Tunnels environment, robots must find and traverse multiple tunnels while moving from the red start positions at the back to the blue goal positions at the front.

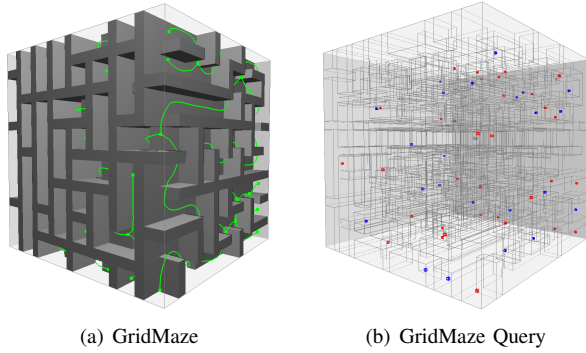


Fig. 8. In the GridMaze environment, robots must move between randomly located starts (red) and goals (blue) within the maze, some of which overlap.

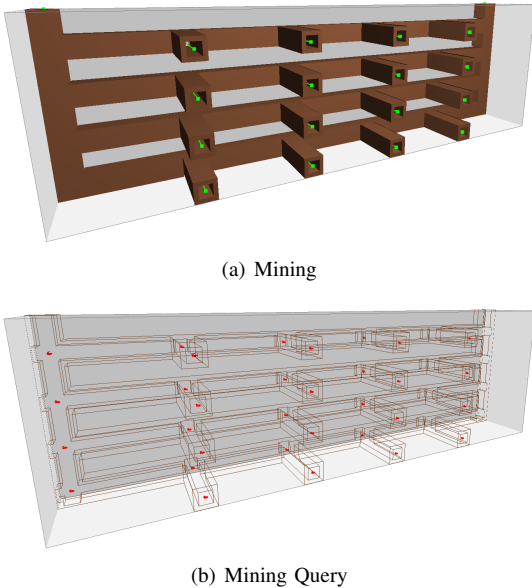


Fig. 9. In the mining environment, robots must swap places with another robot located in an adjacent mine shaft, query locations are shown in red.

run using a computer with an AMD Ryzen 9 7940HS CPU at 4GHz and 32GB of RAM. We run 15 seeds for each scenario. Each method is given 600 seconds to solve a scenario or is considered a failure. We report planning time as well as path cost as given by the makespan.

B. Environments

Here, we describe our experimental environments and explain which aspects of our approach these scenarios are designed to highlight.

1) *Warehouse (Fig. 6)*: The Warehouse environment features a series of narrow aisles. Robots start on the top and bottom of the narrow aisles and must swap places with the robot with which they are vertically aligned. In the holonomic scenario, the width of the narrow passages is approximately 2.5 times the diameter of the disk robots we consider. We additionally run a kinodynamic variant of this scenario with doubled narrow passage widths and rectangular robots (see Sec. V-D). This scenario measures each approach’s ability to efficiently handle narrow passages within the environment.

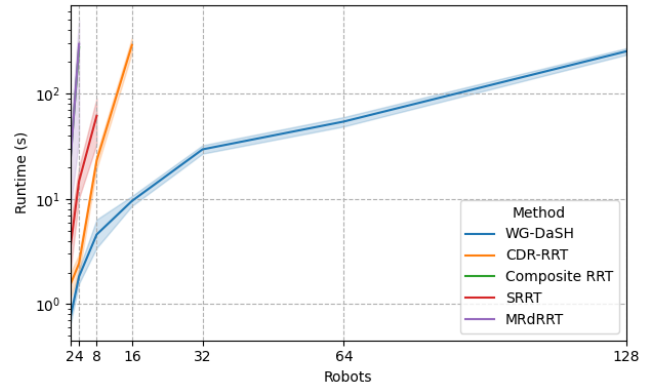


Fig. 10. Average runtime results for the Warehouse scenario. The standard deviation is shown by the shaded region around each line. Data is omitted where all seeds failed.

TABLE I
WAREHOUSE RESULTS. DATA OMITTED WHERE ALL SEEDS FAILED

Method	Robots	Runtime (s)		Cost (s)		Success
		Avg	Std	Avg	Std	
WG-DaSH	2	0.7	0.3	31.6	4.4	100%
CDR-RRT		1.5	0.8	22.3	2.6	100%
SRRT		3.4	3.7	29.8	9.5	100%
Comp. RRT		22.6	24.2	25.7	12.2	100%
MRdRRT		21.6	26.4	82.1	35.2	53.3%
WG-DaSH	4	1.8	0.6	32.8	3.2	100%
CDR-RRT		2.4	1.0	27.6	6.7	100%
SRRT		14.7	9.6	33.2	18.9	86.7%
Comp. RRT		274.0	-	19.2	-	6.7%
MRdRRT		295.0	233.4	107.1	77.4	20.0%
WG-DaSH	8	4.6	3.2	32.5	3.0	100%
CDR-RRT		23.0	8.2	42.2	7.5	100%
SRRT		61.4	40.1	20.9	0.3	13.3%
WG-DaSH	16	9.5	2.1	31.4	3.4	100%
CDR-RRT		288.1	100.2	50.1	7.1	93.3%
WG-DaSH	32	29.5	5.8	34.3	4.0	100%
WG-DaSH	64	54.1	11.4	35.6	2.7	100%
WG-DaSH	128	250.7	29.4	36.6	5.0	60.0%

We highlight Workspace Guided-DaSH’s ability to decompose the problem using topological guidance.

2) *Tunnels (Fig. 7)*: The Tunnels environment is three-dimensional and features several narrow passages that the robots must traverse. Because of the three-dimensional workspace, the size of the planning space becomes very large. This scenario is intended to measure each algorithm’s performance with respect to the geometric complexity, rather than the congestion, of the environment. We consider L-shaped robots with the width of their longest dimension slightly less than half the width of the narrow passages. Each robot must find and traverse multiple narrow passages to reach its goal, but its shortest path does not conflict with any other robot’s.

3) *Mining (Fig. 9)*: The Mining environment is a 3D environment meant to mimic a set of mine shafts. Again, it features several narrow passages; however, here robots must move in close proximity to each other. We use the same robots as the Tunnels environment. We show that Workspace Guided-DaSH is capable of efficiently finding paths for large robot teams in real-world scenarios.

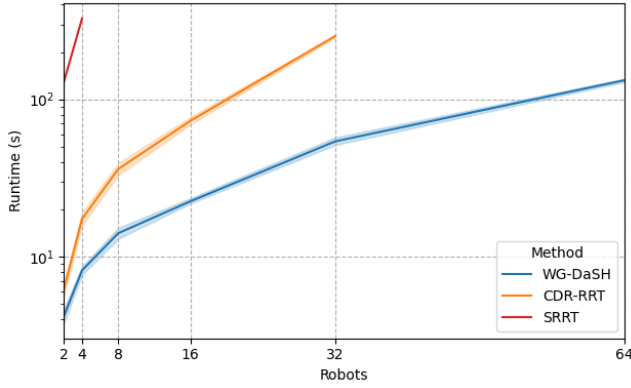


Fig. 11. Average runtime results for the Tunnels scenario. The standard deviation is shown by the shaded region around each line. Data is omitted where all seeds failed.

TABLE II

TUNNELS RESULTS. DATA OMITTED WHERE ALL SEEDS FAILED

Method	Robots	Runtime (s)		Cost (s)		Success
		Avg	Std	Avg	Std	
WG-DaSH	2	4.2	0.9	166.0	5.1	100%
CDR-RRT		6.2	1.1	140.6	11.2	100%
SRRT		129.6	175.0	175.3	26.1	40.0%
WG-DaSH	4	8.2	1.0	158.3	9.0	100%
CDR-RRT		17.3	3.3	152.9	16.4	100%
SRRT		327.0	-	161.7	-	6.7%
WG-DaSH	8	14.1	2.4	159.8	8.4	100%
CDR-RRT		36.0	6.8	156.1	9.0	100%
SRRT		-	-	-	-	-
WG-DaSH	16	22.5	1.9	164.8	9.4	100%
CDR-RRT		73.1	8.5	163.9	16.7	100%
SRRT		-	-	-	-	-
WG-DaSH	32	54.0	6.2	163.0	8.0	100%
CDR-RRT		252.6	10.0	159.8	4.7	93.3%
SRRT		-	-	-	-	-
WG-DaSH	64	132.4	7.0	163.1	6.0	100%

4) *GridMaze* (Fig. 8): The GridMaze environment is a 3D environment featuring several intersecting narrow tunnels intended to elicit high congestion for large groups of robots in addition to geometric complexity. We use a rectangular prism robot whose smallest dimension is slightly less than half the width of the narrow passages. We demonstrate Workspace Guided-DaSH's ability to efficiently find paths for large groups of robots in these congested settings.

C. Workspace Guided-DaSH Results

In the Warehouse scenario (results in Fig. 10 and Tab. I), all methods except MRdRRT achieve a 100% success rate in the 2-robot scenario. However, the methods that do not leverage topological guidance begin to struggle with the 4-robot scenario and most cannot solve the 8-robot scenario. CDR-RRT and SRRT are able to solve up to the 8-robot scenario where the exponential size of the composite space leads to a significant decrease in performance. Workspace Guided-DaSH, like CDR-RRT, sees the benefit of using the skeleton representation to guide planning through narrow passages and the coordination provided by using the composite space of multiple robots. Additionally, by using the workspace to inform the planner when to move between different levels of composition, Workspace Guided-DaSH is able to focus planning within smaller spaces than CDR-RRT, making it

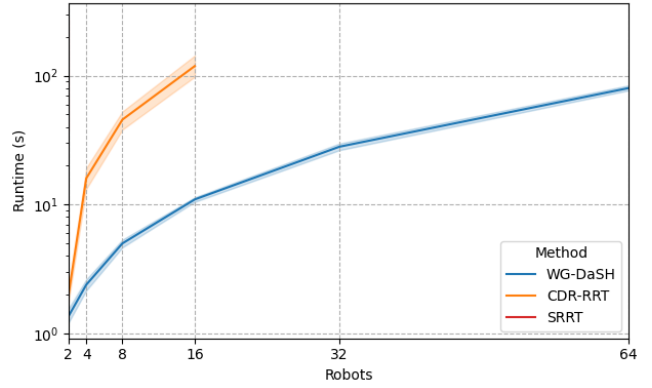


Fig. 12. Average runtime results for the Mining scenario. The standard deviation is shown by the shaded region around each line. Data is omitted where all seeds failed.

TABLE III

MINING RESULTS. DATA OMITTED WHERE ALL SEEDS FAILED

Method	Robots	Runtime (s)		Cost (s)		Success
		Avg	Std	Avg	Std	
WG-DaSH	2	1.3	0.3	125.6	6.5	100%
CDR-RRT		1.9	0.4	113.0	11.7	100%
SRRT		146.8	161.7	131.5	17.5	33.3%
WG-DaSH	4	2.4	0.5	122.6	10.6	100%
CDR-RRT		16.0	6.1	151.2	19.5	100%
SRRT		-	-	-	-	-
WG-DaSH	8	5.0	0.8	132.2	6.7	100%
CDR-RRT		45.7	14.8	160.6	12.9	100%
SRRT		-	-	-	-	-
WG-DaSH	16	11.0	1.0	130.3	5.8	100%
CDR-RRT		118.9	44.3	179.0	17.5	100%
SRRT		-	-	-	-	-
WG-DaSH	32	28.1	3.5	127.6	6.7	100%
WG-DaSH	64	80.2	6.9	124.5	4.5	86.7%

able to plan for significantly larger robot teams, up to 128 robots, within the 600-second time limit.

In the Tunnels environment (results in Fig. 11 and Tab. II), the size of the search space is increased significantly relative to the Warehouse environment since the robot now has six degrees of freedom. Composite RRT and MRdRRT are unable to find a solution for the 2-robot scenario. This is due both to the large size of the search space and the complexity of the environment. SRRT performs better because of its ability to decompose the search space, but struggles with the narrow passages and only one seed was able to solve the 4-robot scenario. Here, the narrow passage problem is exacerbated since the query requires the planner to find and traverse multiple narrow passages. By leveraging skeleton guidance, CDR-RRT and Workspace Guided-DaSH are able to find solutions for larger groups of robots. Searching the composite space, which grows exponentially with the number of robots, hinders CDR-RRT's performance, leaving it unable to solve the 64-robot scenario within the time limit. Workspace Guided-DaSH is able to efficiently find solutions for up to 64 robots within the time limit due to its ability to decompose the planning space.

In the Mining environment (results in Fig. 12 and Tab. III), Composite RRT and MRdRRT are unable to find a solution for the 2-robot scenario due to the large size of the search space and inter-robot conflicts. Similarly, SRRT struggles

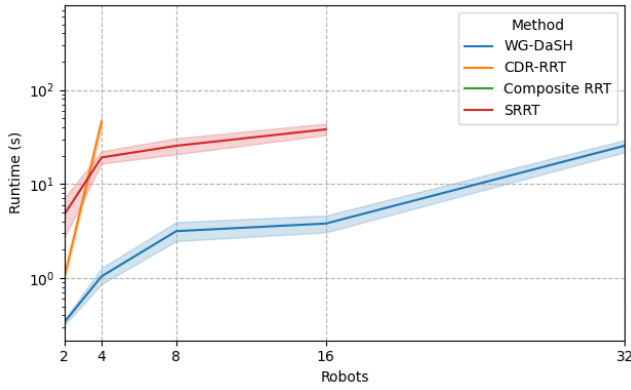


Fig. 13. Average runtime results for the GridMaze scenario. The standard deviation is shown by the shaded region around each line. Data is omitted where all seeds failed. The line for Composite RRT is not visible since it only succeeded for the 2-robot scenario.

TABLE IV
GRIDMAZE RESULTS. DATA OMITTED WHERE ALL SEEDS FAILED

Method	Robots	Runtime (s)		Cost (s)		Success
		Avg	Std	Avg	Std	
WG-DaSH	2	0.3	0.04	44.0	5.5	100%
CDR-RRT		1.0	0.3	63.9	8.3	100%
SRRT		4.7	4.8	30.7	3.8	100%
Comp. RRT		425.0	136.0	59.4	11.5	20.0%
WG-DaSH	4	1.0	0.5	44.2	3.8	100%
CDR-RRT		46.0	17.7	120.6	15.9	100%
SRRT		19.2	6.0	30.9	4.1	100%
WG-DaSH	8	3.2	1.5	42.3	3.3	100%
SRRT		25.5	10.6	32.8	9.7	100%
WG-DaSH	16	3.8	1.6	44.2	4.1	100%
SRRT		38.1	10.8	29.3	2.6	100%
WG-DaSH	32	25.5	7.9	36.3	16.4	93.3%

to find solutions for the 2-robot scenario and cannot solve the 4-robot scenario. By leveraging topological guidance to limit exploration of the composite space, CDR-RRT is able to solve up to the 16-robot scenario. However, it is unable to solve the 32-robot scenario. Workspace Guided-DaSH, by considering the composite space only when necessary, is able to efficiently solve up to the 64-robot scenario within the time limit.

In the 3D GridMaze scenario (results in Fig. 13 and Tab. IV), as a result of the large size of the planning space as well as the difficulty posed by the long curved narrow passages, Composite RRT struggles with the 2-robot scenario and fails to produce a solution for the 4-robot scenario. MRdRRT fails to solve the 2-robot scenario. While CDR-RRT is able to solve the 4-robot scenario, the large size of the composite space prevents it from finding a solution for the 8-robot scenario within the time limit. SRRT benefits from searching a lower-dimensional space when robots are not in conflict, but fails to solve the 32-robot scenario where conflicts become prevalent due to the high level of congestion of the environment. Similar to SRRT, Workspace Guided-DaSH searches lower-dimensional spaces, however, our method also uses the workspace skeleton for conflict resolution. When a conflict is too difficult to be resolved

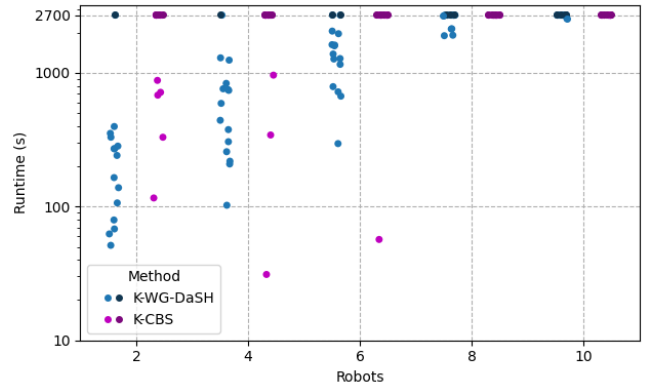


Fig. 14. Average runtime results for the kinodynamic Warehouse scenario. The darker colors indicate seeds that exceeded the time limit of 2700 seconds. Lighter colors show the runtimes of seeds that succeeded to find a path.

TABLE V
KINODYNAMIC WAREHOUSE RESULTS. DATA OMITTED WHERE ALL SEEDS FAILED

Method	Robots	Runtime (s)		Cost (s)		Success
		Avg	Std	Avg	Std	
K-WG-DaSH	2	201.2	119.1	46.7	9.9	93.3%
K-CBS		390.1	365.9	34.4	2.3	46.7%
K-WG-DaSH	4	580.2	376.2	41.9	7.3	93.3%
K-CBS		445.0	473.3	35.1	2.7	20.0%
K-WG-DaSH	6	1261.6	524.5	32.1	14.8	86.7%
K-CBS		56.8	-	33.5	-	6.7%
K-WG-DaSH	8	2147.2	313.1	19.1	16.0	33.3%
K-WG-DaSH	10	2544.7	-	36.5	-	6.7%

quickly via random sampling, we impose constraints on the robots' abstract paths through the workspace which allows us to find conflict-free paths more efficiently. Thus, Workspace Guided-DaSH is able to find solutions up to 32 robots. Although this replanning mechanism sometimes results in slightly higher solution costs relative to other methods, a post-processing trajectory optimization step is generally used in practice to smooth paths.

D. Kinodynamic Experiment Setup

To show the ability of our method to operate on problems with kinodynamic constraints, we use the Kinodynamic RRT 5 as our RRT in the motion hypergraph construction of Workspace Guided-DaSH. Our kinodynamic steering function selects the best control out of 50 randomly sampled options and has a maximum applied duration of 50 timesteps.

We compare the performance of our Kinodynamic Workspace Guided-DaSH against Kinodynamic CBS [29] as it is an unguided multi-robot kinodynamic motion planning method which uses Conflict-Based Search [36] as a high-level planner to resolve conflicts with kinodynamic RRT as the low-level planner. The dynamics are integrated using the 4th-order Runge-Kutta (RK4) method [37]. K-CBS utilizes a merge bound to inform the high-level search of robots which are repeatedly in conflict with each other after re-planning, drawn from an extension of CBS: Meta-agent CBS [38]. Once this merge bound is reached for a set of robots, the

planner merges the robots into a composite robot. The idea is that, if the robots are constantly in conflict with each other, then their coordination is tightly coupled and planning in the composite space will enable the planner to capture the level of coordination needed to find a solution for the set of robots. The authors of Meta-agent CBS [38], state that if the environment consists of narrow corridors where high levels of coordination are required, the merge bound should be set low so the planner can quickly increase the level of coordination being considered to match the problem difficulty. Following his insight, we use a merge bound of 3 in our experiments to allow the planner to quickly match the level of coordination needed for the challenging problems we are considering. Both methods were implemented in the open-source Parasol Planning Library and experiments were run using a computer with an Intel i9-14900K CPU at 6GHz and 64GB of RAM. Each method was given 45 minutes to find a solution to each problem.

As in [29], all robots use 2nd-order car dynamics:

$$\dot{x} = v \cos \theta, \quad \dot{y} = v \sin \theta, \quad \dot{\theta} = \frac{v}{l} \tan \phi, \quad \dot{v} = a, \quad \dot{\phi} = \gamma \quad (2)$$

with x and y defining the position of the robot and θ defining the orientation. We let v define the velocity, ϕ define the steering angle of the front wheels of the car. a is the first control input representing acceleration, and γ as the second control input representing the steering rate. Additionally, we keep the same robot shapes as in [29] but scale down the size of the robots to fit the environment, rectangular robots with length $l = 0.35$ and width $w = 0.25$.

E. Kinodynamic Workspace Guided-DaSH Results

As detailed in Sec. V-B.1, we run a kinodynamic variant of the Warehouse scenario. In order to account for the increased problem difficulty imposed by kinodynamic constraints, we increased the size of the narrow passages in the environment. Results are shown in Figure 14 and Table V.

In the kinodynamic warehouse environment, K-WG-DaSH can find solutions for problems with up to 6 robots fairly consistently while K-CBS begins to struggle at 4 robots. In the 2 robot scenario, K-WG-DaSH maintains a high success rate with a lower planning time at the expense of a higher path cost as opposed to K-CBS which is inconsistent at finding solutions with a higher planning time but with a lower path cost. At 4 robots, K-CBS sees a significant drop off in success rate, while K-WG-DaSH maintains it's high success rate. When 6 robots are considered, K-CBS has an extremely difficult time finding solutions and when 8 or 10 robots are considered, it cannot find any solutions in the time limit. K-WG-DaSH sees a slight drop off in success rate at 6 robots, and a larger drop off at 8 and 10 robots, however, it is able to find at least one solution. We argue that the addition of guidance over when to coordinate and topological guidance providing where to go is the reason for the improved success rate and scalability of K-WG-DaSH over K-CBS.

VI. CONCLUSION AND FUTURE WORK

In this work, we present both the Guided-DaSH framework for hybrid multi-robot planning and an application of this framework to mobile robot MRMP in congested environments. Our adapted framework builds off of a state-of-the-art hybrid planning framework, DaSH, using guidance to enable its application to a wider range of multi-robot planning problems which lack the highly structured search space seen in previous DaSH methods. Additionally, we add support for kinodynamic planning via a modified conflict resolution structure, which also boosts the scalability of our framework by eliminating unnecessary work when finding motion solutions.

Our application of Guided-DaSH to mobile robot MRMP in congested environments, Workspace Guided-DaSH leverages topological guidance in multiple ways, both to inform how to move between different levels of composition during planning and to guide sampling through narrow passages in the workspace. By using knowledge of the workspace, our method is able to efficiently find paths for robot groups of size up to an order of magnitude larger than existing state-of-the-art methods. Building off of this work, we plan to explore the use of different kinodynamic low-level motion planners which plan more intelligently for multi-robot systems by interleaving sampling-based planning and trajectory optimization [39]. Additionally, we plan to explore using parallel computing to further improve the performance of this method, taking advantage of the hypergraph's ability to naturally decompose the multi-robot planning problems.

REFERENCES

- [1] G. Sanchez and J.-C. Latombe, "Using a prm planner to compare centralized and decoupled planning for multi-robot systems," in *Proc. IEEE Int. Conf. Robot. Autom. (ICRA)*, vol. 2, 2002, pp. 2112–2119.
- [2] I. Solis, J. Motes, R. Sandström, and N. M. Amato, "Representation-optimal multi-robot motion planning using conflict-based search," *IEEE Robotics and Automation Letters*, vol. 6, no. 3, pp. 4608–4615, 2021.
- [3] G. Wagner and H. Choset, "M*: A complete multirobot path planning algorithm with performance bounds," in *Proc. IEEE Int. Conf. Intel. Rob. Syst. (IROS)*, 2011, pp. 3260–3267.
- [4] W. Hönig, J. A. Preiss, T. K. S. Kumar, G. S. Sukhatme, and N. Ayanian, "Trajectory planning for quadrotor swarms," *IEEE Transactions on Robotics*, vol. 34, no. 4, pp. 856–869, 2018.
- [5] J. Motes, T. Chen, T. Bretl, M. M. Aguirre, and N. M. Amato, "Hypergraph-based multi-robot task and motion planning," *IEEE Transactions on Robotics*, vol. 39, no. 5, pp. 4166–4186, 2023.
- [6] J. Denny, R. Sandström, A. Bregger, and N. M. Amato, "Dynamic region-biased rapidly-exploring random trees," in *Alg. Found. Robot. XII*. Springer, 2020, (WAFR '16).
- [7] R. Sandstrom, D. Uwacu, J. Denny, and N. M. Amato, "Topology-guided roadmap construction with dynamic region sampling," *IEEE Robotics and Automation Letters*, vol. 5, no. 4, pp. 6161–6168, 2020.
- [8] M. Rickert, A. Sieverling, and O. Brock, "Balancing exploration and exploitation in sampling-based motion planning," *IEEE Transactions on Robotics*, vol. 30, no. 6, pp. 1305–1317, 2014.
- [9] E. Plaku, L. Kavraki, and M. Vardi, "Motion planning with dynamics by a synergistic combination of layers of planning," *IEEE Trans. Robot.*, vol. 26, no. 3, pp. 469–482, June 2010.
- [10] C. McBeth, J. Motes, D. Uwacu, M. Morales, and N. M. Amato, "Scalable multi-robot motion planning for congested environments with topological guidance," *IEEE Robotics and Automation Letters*, vol. 8, no. 11, pp. 6867–6874, 2023.

- [11] J. T. Schwartz and M. Sharir, "On the "piano movers" problem. ii. general techniques for computing topological properties of real algebraic manifolds," *Advances in applied Mathematics*, vol. 4, no. 3, pp. 298–351, 1983.
- [12] J. F. Canny, *The Complexity of Robot Motion Planning*. Cambridge, MA: MIT Press, 1988.
- [13] L. E. Kavraki, P. Švestka, J. C. Latombe, and M. H. Overmars, "Probabilistic roadmaps for path planning in high-dimensional configuration spaces," *IEEE Trans. Robot. Automat.*, vol. 12, no. 4, pp. 566–580, Aug. 1996.
- [14] S. M. Lavalle, "Rapidly-exploring random trees: A new tool for path planning," Iowa State University, Tech. Rep. 11, 1998.
- [15] C. Holleman and L. E. Kavraki, "A framework for using the workspace medial axis in prm planners," in *Proc. IEEE Int. Conf. Robot. Autom. (ICRA)*, vol. 2, San Francisco, CA, 2000, pp. 1408–1413.
- [16] J. D. Marble and K. E. Bekris, "Asymptotically near-optimal planning with probabilistic roadmap spanners," *IEEE Trans. Robot.*, vol. 29, pp. 432–444, 2013.
- [17] K. Solovey, O. Salzman, and D. Halperin, "Finding a needle in an exponential haystack: Discrete rrt for exploration of implicit roadmaps in multi-robot motion planning," *The International Journal of Robotics Research*, vol. 35, no. 5, pp. 501–513, 2016.
- [18] A. Dobson, K. Solovey, R. Shome, D. Halperin, and K. E. Bekris, "Scalable asymptotically-optimal multi-robot motion planning," in *2017 international symposium on multi-robot and multi-agent systems (MRS)*. IEEE, 2017, pp. 120–127.
- [19] R. Shome, K. Solovey, A. Dobson, D. Halperin, and K. E. Bekris, "drrt*: Scalable and informed asymptotically-optimal multi-robot motion planning," *Autonomous Robots*, vol. 44, no. 3, pp. 443–467, 2020.
- [20] G. Wagner, M. Kang, and H. Choset, "Probabilistic path planning for multiple robots with subdimensional expansion," in *2012 IEEE International Conference on Robotics and Automation*, 2012, pp. 2886–2892.
- [21] B. Lau, C. Sprunk, and W. Burgard, "Kinodynamic motion planning for mobile robots using splines," in *2009 IEEE/RSJ International Conference on Intelligent Robots and Systems*. IEEE, 2009, pp. 2427–2433.
- [22] M. Pivtoraiko and A. Kelly, "Kinodynamic motion planning with state lattice motion primitives," in *2011 IEEE/RSJ International Conference on Intelligent Robots and Systems*. IEEE, 2011, pp. 2172–2179.
- [23] B. Sakkak, L. Bascetta, G. Ferretti, and M. Prandini, "Sampling-based optimal kinodynamic planning with motion primitives," *Autonomous Robots*, vol. 43, no. 7, pp. 1715–1732, 2019.
- [24] D. Hsu, R. Kindel, J.-C. Latombe, and S. Rock, "Randomized kinodynamic motion planning with moving obstacles," *The International Journal of Robotics Research*, vol. 21, no. 3, pp. 233–255, 2002.
- [25] A. Perez, R. Platt, G. Konidaris, L. Kaelbling, and T. Lozano-Perez, "Lqr-rrt*: Optimal sampling-based motion planning with automatically derived extension heuristics," in *2012 IEEE International Conference on Robotics and Automation*. IEEE, 2012, pp. 2537–2542.
- [26] J. Van Den Berg, P. Abbeel, and K. Goldberg, "Lqg-mp: Optimized path planning for robots with motion uncertainty and imperfect state information," 2011.
- [27] S. Karaman and E. Frazzoli, "Optimal kinodynamic motion planning using incremental sampling-based methods," in *49th IEEE conference on decision and control (CDC)*. IEEE, 2010, pp. 7681–7687.
- [28] D. J. Webb and J. v. d. Berg, "Kinodynamic rrt*: Optimal motion planning for systems with linear differential constraints," *arXiv preprint arXiv:1205.5088*, 2012.
- [29] J. Kottinger, S. Almagor, and M. Lahijanian, "Conflict-based search for multi-robot motion planning with kinodynamic constraints," in *2022 IEEE/RSJ International Conference on Intelligent Robots and Systems (IROS)*. IEEE, 2022, pp. 13 494–13 499.
- [30] H. Blum, "A transformation for extracting new descriptors of shape," in *Models for Perception of Speech and Visual Form*, W. Wathen-Dunn, Ed. Cambridge, MA: MIT Press, 1967.
- [31] G. Reeb, "Sur les points singuliers d'une forme de pfaff completement integrable ou d'une fonction numerique," *Comptes Rendus Acad. Sciences Paris*, no. 222, pp. 847–849, 1946.
- [32] A. Tagliasacchi, I. Alhashim, M. Olson, and H. Zhang, "Mean curvature skeletons," *Computer Graphics Forum*, vol. 31, pp. 1735–1744, 08 2012.
- [33] D. T. Lee, "Medial axis transformation of a planar shape," *IEEE Transactions on Pattern Analysis and Machine Intelligence*, vol. PAMI-4, no. 4, pp. 363–369, 1982.
- [34] D. Uwacu, A. Yammanuru, M. Morales, and N. M. Amato, "Hierarchical planning with annotated skeleton guidance," *IEEE Robotics and Automation Letters*, vol. 7, no. 4, pp. 11 055–11 061, 2022.
- [35] G. Gallo, G. Longo, S. Pallottino, and S. Nguyen, "Directed hypergraphs and applications," *Discrete Applied Mathematics*, vol. 42, no. 2, pp. 177–201, 1993. [Online]. Available: <https://www.sciencedirect.com/science/article/pii/0166218X9390045P>
- [36] G. Sharon, R. Stern, A. Felner, and N. R. Sturtevant, "Conflict-based search for optimal multi-agent pathfinding," *Artificial Intelligence*, vol. 219, pp. 40–66, 2015.
- [37] R. Burden, R. Burden, and J. Faires, *Numerical Analysis*, ser. Numerical Analysis. Brooks/Cole, 2001, no. v. 1. [Online]. Available: <https://books.google.com/books?id=7ofAQgAACAAJ>
- [38] G. Sharon, R. Stern, A. Felner, and N. Sturtevant, "Meta-agent conflict-based search for optimal multi-agent path finding," in *Proceedings of the International Symposium on Combinatorial Search*, vol. 3, no. 1, 2012, pp. 97–104.
- [39] A. Moldagalieva, J. Ortiz-Haro, M. Toussaint, and W. Hönig, "db-cbs: Discontinuity-bounded conflict-based search for multi-robot kinodynamic motion planning," *arXiv preprint arXiv:2309.16445*, 2023.